

HIF-1 α is over-expressed in leukemic cells from TP53-disrupted patients and is a promising therapeutic target in chronic lymphocytic leukemia

Valentina Griggio,^{1,2*} Candida Vitale,^{1,2*} Maria Todaro,^{1,2} Chiara Riganti,³ Joanna Kopecka,³ Chiara Salvetti,^{1,2} Riccardo Bomben,⁴ Michele Dal Bo,⁴ Daniela Magliulo,⁵ Davide Rossi,⁶ Gabriele Pozzato,⁷ Lisa Bonello,² Monia Marchetti,⁸ Paola Omedè,¹ Ahad Ahmed Kodipad,⁹ Luca Laurenti,¹⁰ Giovanni Del Poeta,¹¹ Francesca Romana Mauro,¹² Rosa Bernardi,⁵ Thorsten Zenz,¹³ Valter Gattei,⁴ Gianluca Gaidano,⁹ Robin Foà,¹² Massimo Massaia,¹⁴ Mario Boccadoro^{1,2} and Marta Coscia^{1,2}

¹Division of Hematology, A.O.U. Città della Salute e della Scienza di Torino, Turin, Italy; ²Department of Molecular Biotechnology and Health Sciences, University of Turin, Turin, Italy; ³Department of Oncology, University of Turin, Turin, Italy; ⁴Clinical and Experimental Onco-Hematology Unit, CRO Aviano National Cancer Institute, Aviano, Italy; ⁵Division of Experimental Oncology, IRCCS San Raffaele Scientific Institute, Milan, Italy; ⁶Department of Hematology, Oncology Institute of Southern Switzerland and Institute of Oncology Research, Bellinzona, Switzerland; ⁷Department of Internal Medicine and Hematology, Maggiore General Hospital, University of Trieste, Trieste, Italy; ⁸Hematology Day Service, Oncology SOC, Hospital Cardinal Massaia, Asti, Italy; ⁹Division of Hematology, Department of Translational Medicine, University of Eastern Piedmont, Novara, Italy; ¹⁰Fondazione Policlinico Universitario Agostino Gemelli, Rome, Italy; ¹¹Division of Hematology, S. Eugenio Hospital and University of Tor Vergata, Rome, Italy; ¹²Hematology, Department of Translational and Precision Medicine, Sapienza University, Policlinico Umberto I, Rome, Italy; ¹³Department of Medical Oncology and Hematology, University Hospital and University of Zurich, Zurich, Switzerland and ¹⁴Hematology Unit, ASO Santa Croce e Carle, Cuneo, Italy

*VG and CV contributed equally to this study.

©2020 Ferrata Storti Foundation. This is an open-access paper. doi:10.3324/haematol.2019.217430

Received: February 1, 2019.

Accepted: July 4, 2019.

Pre-published: July 9, 2019.

Correspondence: MARTA COSCIA - marta.coscia@unito.it

Supplemental Information

Article title: HIF-1 α is overexpressed in leukemic cells from TP53-disrupted patients and is a promising therapeutic target in CLL

Running Head: HIF-1 α in TP53-disrupted CLL Cells

Authors: Valentina Griggio^{1,2}, Candida Vitale^{1,2}, Maria Todaro^{1,2}, Chiara Riganti³, Joanna Kopecka³, Chiara Salvetti^{1,2}, Riccardo Bomben⁴, Michele Dal Bo⁴, Daniela Magliulo⁵, Davide Rossi⁶, Gabriele Pozzato⁷, Lisa Bonello², Monia Marchetti⁸, Paola Omedè¹, Ahad Ahmed Kodipad⁹, Luca Laurenti¹⁰, Giovanni Del Poeta¹¹, Francesca Romana Mauro¹², Rosa Bernardi⁵, Thorsten Zenz¹³, Valter Gattei⁴, Gianluca Gaidano⁹, Robin Foà¹², Massimo Massaia¹⁴, Mario Boccardo^{1,2} and Marta Coscia^{1,2}

Affiliations:

¹Division of Hematology, University of Torino, A.O.U. Città della Salute e della Scienza di Torino, Turin, Italy

²Department of Molecular Biotechnology and Health Sciences, University of Torino, Torino, Italy

³Department of Oncology, University of Torino, Turin, Italy

⁴Clinical and Experimental Onco-Hematology Unit, CRO Aviano National Cancer Institute, Aviano, Italy

⁵Division of Experimental Oncology, IRCCS San Raffaele Scientific Institute, Milan, Italy;

⁶Department of Hematology, Oncology Institute of Southern Switzerland and Institute of Oncology Research, Bellinzona, Switzerland

⁷Department of Internal Medicine and Hematology, Maggiore General Hospital, University of Trieste, Trieste, Italy

⁸Hematology Day Service, Oncology SOC, Hospital Cardinal Massaia, Asti, Italy

⁹Division of Hematology, Department of Translational Medicine, University of Eastern Piedmont, Novara, Italy

¹⁰Fondazione Policlinico Universitario Agostino Gemelli, Rome, Italy

¹¹Division of Hematology, S. Eugenio Hospital and University of Tor Vergata, Rome, Italy

¹²Hematology, Department of Translational and Precision Medicine, Sapienza University, Policlinico Umberto I, Rome, Italy

¹³Department of Medical Oncology and Hematology, University Hospital and University of Zurich, Zurich, Switzerland

¹⁴Hematology Unit, ASO Santa Croce e Carle, Cuneo, Italy

V.Griggio and C.V. contributed equally to this study.

Supplemental Methods

Cells preparation and culture

PBMC were separated using Ficoll-Hypaque (Sigma-Aldrich) and stained with anti-CD19 PerCP Vio700 and anti-CD5-APC antibodies (Miltenyi Biotec, Bologna, Italy). When the CD19+/CD5+ cells were < 90%, CLL cells were purified by negative selection and cultured in RPMI-1640 medium with 10% of fetal bovine serum (FBS) and penicillin/streptomycin. B lymphocytes from healthy donors were purified by positive selection using anti-CD19 micro beads (Miltenyi Biotec). Del(17p) was assessed by *fluorescence in situ hybridization* and the presence of *TP53* gene mutations was evaluated by Sanger sequencing. Immunoglobulin heavy chain variable region gene (IGHV) mutational status was assessed as already described¹. Cell lines used in the experiments (i.e. Séraphine, Granta-519 and M2-10B4) were maintained in RPMI-1640 or DMEM medium with 10% fetal bovine serum, glutamine and antibiotics at 37 °C, 5% CO₂. A humidified hypoxia incubator chamber was used for hypoxic cultures.

Antibodies used for flow cytometry

Two- and three-color flow cytometry was performed with FACSCalibur and CELLQuest software (Becton Dickinson, Mountain View, CA) and with BD Accuri C6 flow cytometer (BD Biosciences). Data were analyzed with FlowJo software (Tree Star, Inc, Ashland, OR). Antibodies used for flow cytometry were: anti-CD19-PE (BD Biosciences, San José, CA), anti-CD19-PerCP Vio700 (Miltenyi Biotec), anti-CD5-APC (Miltenyi Biotec).

Western blot analysis

Cytosolic and nuclear protein extracts were obtained using the Nuclear Extract Kit (Active Motif, La Hulpe) following the manufacturer's instructions. Lysates were resolved by SDS-PAGE and transferred to nitrocellulose membranes (Bio-Rad, Hercules, CA). The following antibodies were used: anti-HIF-1 α (BD Biosciences, San José, CA), anti-ELK3

(Sigma Aldrich); anti-pVHL (EuroClone Spa, Milano); anti p(Thr202/Tyr204, Thr185/Tyr187)-ERK1–2 (Millipore, Bedford, MA); anti-ERK1-2 (Millipore); anti-RAS (Millipore); anti-RHOA (Santa Cruz Biotechnology Inc., Santa Cruz, CA) antibody anti-p(Ser 473)AKT (Millipore); anti-AKT (Millipore); anti-ACTIN (Sigma Aldrich), anti-GAPDH, anti-TUBULIN and anti-TATA-box binding protein (TBP) (Santa Cruz Biotechnology Inc.) used as control of equal protein loading for cytosolic and nuclear fractions, followed by the secondary peroxidase-conjugated antibodies (Bio-Rad, Hercules, CA). To exclude nuclei-cytosol contamination, we verified that GAPDH and TBP were always undetected in nuclear and cytosolic fractions, respectively (not shown). Blot images were acquired with a ChemiDocTM Touch Imaging System device (Bio-Rad Laboratories). Densitometric analysis was performed with the ImageJ software (NIH, Bethesda, MD).

RNA extraction and quantitative real-time PCR (qRT-PCR)

Total RNA was extracted and reverse transcribed as described². The qRT-PCR was performed with the iTaqTM Universal SYBR[®] Green Supermix (Bio-Rad). The primer sequences were designed with the qPrimerDepot software (<http://primerdepot.nci.nih.gov/>). The primer sequences were: *HIF-1A*: 5'-GGCTGCATCTCGAGACTTT-3'; 5'-GAAGACATCGCGGGGAC; *ENO1*: 5'-GCTCCGGGACAATGATAAGA-3', 5'-TCCATCCATCTCGATCATCA-3', *GAPDH*: 5'-GAAGGTGAAGGTCGGAGT-3', 5'-CATGGTGGAAATCATATTGGAA-3'; *VEGF*: 5'-ATCTTCAAGCCATCCTGTGTGC-3', 5'-GCTCACCGCCTCGGCTTGT-3'. The comparative CT method was used to calculate *HIF-1 α* , *GLUT1*, *ENO1* and *VEGF* expression relative to the *GAPDH* product, used as a housekeeping gene, with the Bio-Rad Software Gene Expression Quantitation.

RAS and RHOA activity

The isoprenylated membrane-associated RAS or RHOA proteins and the non-

isoprenylated cytosolic forms were detected as previously described². Total RAS and RHOA proteins were analyzed by WB; Briefly, the GTP-bound fraction, taken as an index of active G-proteins was measured, using a pull-down assay (with the RAF-1-GST fusion protein, agarose beads-conjugates, Millipore, Bedford, MA) and an ELISA assay (with the G-LISA™ RHOA Activation Assay Biochem Kit, Cytoskeleton Inc, Denver, CO), respectively.

Kinase inhibitors titration and kinase activity

For kinase inhibitors titration experiments we exposed CLL cells (10^6 /mL) for 48 hours to PD98059, LY249002 and Y27632 at indicated increasing concentrations. ERK1-2, AKT and RHOA kinases activity was measured by spectrophotometric methods, using the CycLex RHO Kinase Assay Kit (CycLex, Nagano), the MAP Kinase/Erk Assay Kit (Millipore, Bedford, MA) and the AKT Kinase Activity Assay Kit (Abcam, Cambridge), as per manufacturer's instructions.

Cell viability assay

Cell viability was evaluated by flow cytometry using with Annexin-V/Propidium Iodide (Ann-V/PI) staining with the MEBCYTO-Apoptosis Kit (MBL Medical and Biological Laboratories, Naka-ku Nagoya). Normalized cell viability was arbitrarily defined as the ratio between the percentage of AnnV-/PI- CLL cells cultured in the presence of F-ara-A and the percentage of AnnV-/PI- CLL cells that were left untreated. CLL cells characterized by a normalized cell viability ≥ 0.5 were defined as *fludarabine-resistant*, otherwise, CLL cells were considered *fludarabine-sensitive*.

Table 1. Summary of genetic patient characteristics and treatment status

Unique Patient Number (UPN)	TP53 subset	del(17)p, clone size in %	TP53 ^{mut} , allele frequency in %	IGHV mutational status	Previous Treatment
UPN01	TP53 ^{dis}	neg	mut, 84	M	y
UPN02	TP53 ^{dis}	42	mut, 83	UM	y
UPN03	TP53 ^{dis}	85	mut, 83	UM	n
UPN04	TP53 ^{dis}	80	mut, 79	UM	n
UPN05	TP53 ^{dis}	neg	mut, 75	UM	y
UPN06	TP53 ^{dis}	79	mut, 86	M	n
UPN07	TP53 ^{dis}	neg	mut, nd	UM	y
UPN08	TP53 ^{dis}	nd	mut, nd	M	nd
UPN09	TP53 ^{dis}	87	mut, 81	UM	n
UPN10	TP53 ^{dis}	neg	mut, 88	M	y
UPN11	TP53 ^{dis}	69	mut, 61	UM	y
UPN12	TP53 ^{dis}	neg	mut, 36	M	n
UPN13	TP53 ^{dis}	neg	mut, 50	M	n
UPN14	TP53 ^{dis}	24	mut, 37	UM	y
UPN15	TP53 ^{dis}	monosomy 17	mut, 50	UM	y
UPN16	TP53 ^{dis}	96	mut, 67	nd	n
UPN17	TP53 ^{dis}	neg	mut, 50	UM	y
UPN18	TP53 ^{dis}	53	mut, 31	UM	n
UPN19	TP53 ^{dis}	20	mut, 92	UM	y
UPN20	TP53 ^{dis}	88	nd	UM	n
UPN21	TP53 ^{dis}	21	mut, 25	UM	n
UPN22	TP53 ^{dis}	46	mut, 51	UM	y
UPN23	TP53 ^{dis}	70	nd	nd	y
UPN24	TP53 ^{dis}	neg	mut, 34	M	y
UPN25	TP53 ^{dis}	12	mut, 12	UM	y
UPN26	TP53 ^{dis}	neg	mut, nd	M	y
UPN27	TP53 ^{dis}	82	mut, nd	M	n
UPN28	TP53 ^{dis}	80	mut, 63	UM	y
UPN29	TP53 ^{dis}	68	mut, 75	UM	y
UPN30	TP53 ^{dis}	nd	mut, 73	nd	n
UPN31	TP53 ^{dis}	69	mut, 64	UM	n
UPN32	TP53 ^{dis}	neg	mut, nd	UM	y

UPN33	TP53 ^{dis}	43	mut, 25	M	nd
UPN34	TP53 ^{dis}	neg	mut, nd	UM	n
UPN35	TP53 ^{dis}	91	wt	M	n
UPN36	TP53 ^{dis}	59	wt	nd	n
UPN37	TP53 ^{dis}	50	wt	UM	y
UPN38	TP53 ^{dis}	50	wt	UM	y
UPN39	TP53 ^{dis}	46	wt	M	y
UPN40	TP53 ^{dis}	45	wt	M	n
UPN41	TP53 ^{wt}	neg	wt	M	y
UPN42	TP53 ^{wt}	neg	wt	M	n
UPN43	TP53 ^{wt}	neg	wt	UM	n
UPN44	TP53 ^{wt}	neg	wt	UM	n
UPN45	TP53 ^{wt}	neg	wt	M	y
UPN46	TP53 ^{wt}	neg	wt	M	y
UPN47	TP53 ^{wt}	neg	wt	M	y
UPN48	TP53 ^{wt}	neg	wt	UM	n
UPN49	TP53 ^{wt}	neg	wt	UM	n
UPN50	TP53 ^{wt}	neg	wt	M	n
UPN51	TP53 ^{wt}	neg	wt	UM	n
UPN52	TP53 ^{wt}	neg	wt	UM	y
UPN53	TP53 ^{wt}	neg	wt	UM	n
UPN54	TP53 ^{wt}	neg	wt	UM	n
UPN55	TP53 ^{wt}	neg	wt	UM	n
UPN56	TP53 ^{wt}	neg	wt	M	n
UPN57	TP53 ^{wt}	neg	wt	UM	n
UPN58	TP53 ^{wt}	neg	wt	UM	n
UPN59	TP53 ^{wt}	neg	wt	M	n
UPN60	TP53 ^{wt}	neg	wt	UM	y
UPN61	TP53 ^{wt}	neg	wt	M	n
UPN62	TP53 ^{wt}	neg	wt	M	n
UPN63	TP53 ^{wt}	neg	wt	M	y
UPN64	TP53 ^{wt}	neg	wt	UM	n
UPN65	TP53 ^{wt}	neg	wt	UM	n
UPN66	TP53 ^{wt}	neg	wt	UM	n
UPN67	TP53 ^{wt}	neg	wt	M	n
UPN68	TP53 ^{wt}	neg	wt	M	n
UPN69	TP53 ^{wt}	neg	wt	UM	n
UPN70	TP53 ^{wt}	neg	wt	nd	n

UPN71	TP53 ^{wt}	neg	wt	M	y
UPN72	TP53 ^{wt}	neg	wt	UM	n
UPN73	TP53 ^{wt}	neg	wt	UM	n
UPN74	TP53 ^{wt}	neg	wt	M	n
UPN75	TP53 ^{wt}	neg	wt	M	n
UPN76	TP53 ^{wt}	neg	wt	UM	n
UPN77	TP53 ^{wt}	neg	wt	UM	n
UPN78	TP53 ^{wt}	neg	wt	M	n
UPN79	TP53 ^{wt}	neg	wt	M	n
UPN80	TP53 ^{wt}	neg	wt	UM	n
UPN81	TP53 ^{wt}	neg	wt	M	y
UPN82	TP53 ^{wt}	neg	wt	M	n
UPN83	TP53 ^{wt}	neg	wt	M	n
UPN84	TP53 ^{wt}	neg	wt	M	n
UPN85	TP53 ^{wt}	neg	wt	nd	n
UPN86	TP53 ^{wt}	neg	wt	UM	n
UPN87	TP53 ^{wt}	neg	wt	UM	n
UPN88	TP53 ^{wt}	neg	wt	M	n
UPN89	TP53 ^{wt}	neg	wt	M	n
UPN90	TP53 ^{wt}	neg	wt	UM	n
UPN91	TP53 ^{wt}	neg	wt	nd	n
UPN92	TP53 ^{wt}	neg	wt	UM	n
UPN93	TP53 ^{wt}	neg	wt	UM	n
UPN94	TP53 ^{wt}	neg	wt	nd	n
UPN95	TP53 ^{wt}	neg	wt	UM	n
UPN96	TP53 ^{wt}	neg	wt	M	n
UPN97	TP53 ^{wt}	neg	wt	UM	n
UPN98	TP53 ^{wt}	neg	wt	UM	y
UPN99	TP53 ^{wt}	neg	wt	UM	n
UPN100	TP53 ^{wt}	neg	wt	UM	y
UPN101	TP53 ^{wt}	neg	wt	nd	n
UPN102	TP53 ^{wt}	neg	wt	M	n

Abbreviations

Del(17)p	chromosome 17p13 deletion
neg	negative, <10% del(17p)
TP53 ^{mut}	TP53 gene mutation
mut	presence of TP53 gene mutation
wt	wild type, absence of TP53 gene mutation
nd	not determined
IGHV	Immunoglobulin heavy chain variable region genes

M	IGHV mutated
UM	IGHV unmutated

Supplemental Figures

Supplemental Figure 1

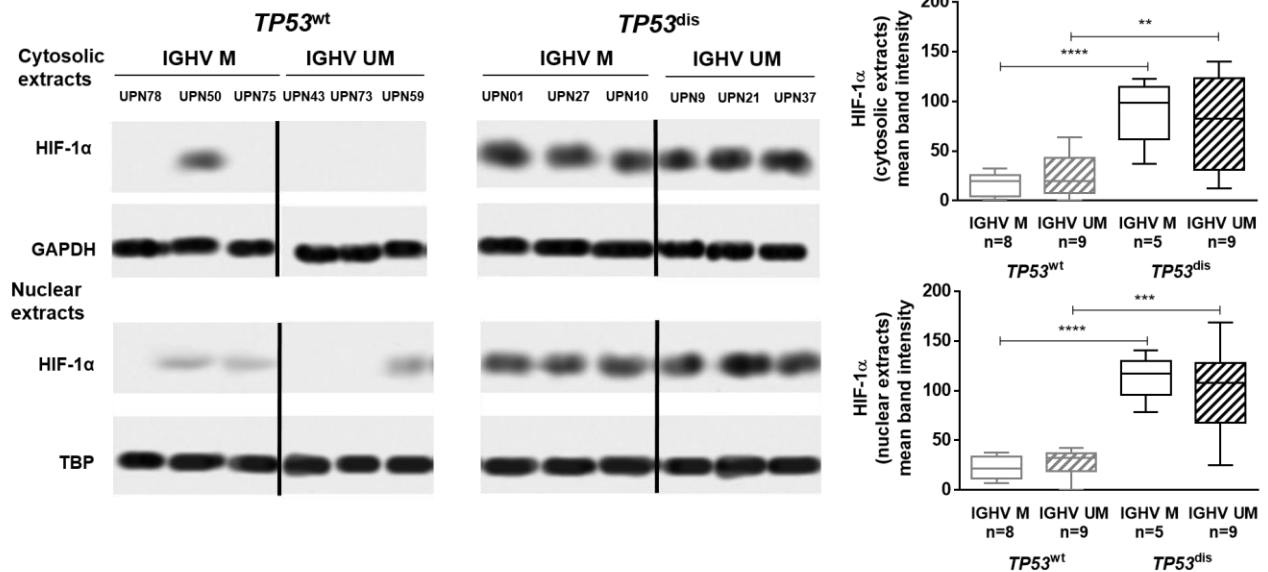
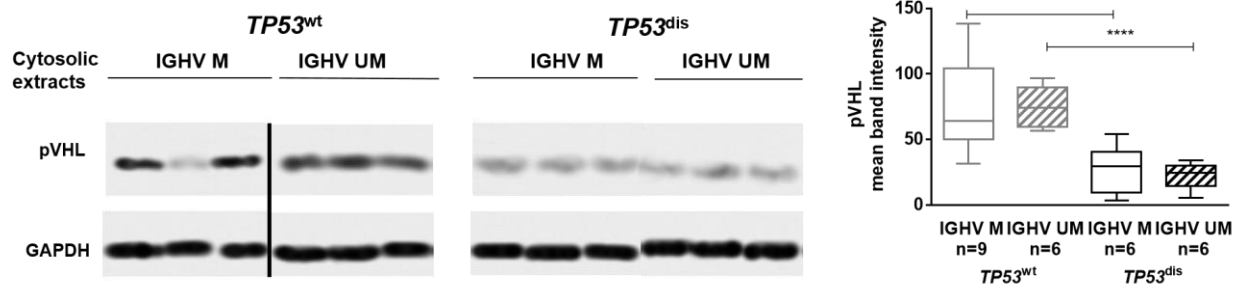


Figure S1. The association between HIF-1 α expression and the *TP53* status is not influenced by the IGHV mutational status. The expression of HIF-1 α was measured in *TP53^{wt}* and *TP53^{dis}* CLL cells, accounting for the IGHV mutational status. *TP53^{wt}* CLL included 8 IGHV M and 9 IGHV UM samples, and *TP53^{dis}* CLL included 5 IGHV M and 8 IGHV UM samples. A representative blot is shown, together with Unique Patients Number (UPN) and cumulative band intensity data obtained from the analysis of the four subsets (i.e. *TP53^{wt}/IGHV M*, *TP53^{wt}/IGHV UM*, *TP53^{dis}/IGHV M* and *TP53^{dis}/IGHV UM* CLL patients). Box plots represent median values and 25%-75% percentiles, whiskers represent minimum and maximum values of band intensity for each group. Vertical lines have been inserted to indicate repositioned gel lanes. **** $p < 0.0001$, *** $p < 0.001$, ** $p < 0.01$.

Supplemental Figure 2

**Figure S2. The expression of pVHL is not influenced by IGHV mutational status.**

The expression of pVHL was measured in $TP53^{wt}$ and $TP53^{dis}$ CLL cells, accounting for the IGHV mutational status. $TP53^{wt}$ CLL included 9 IGHV M and 6 IGHV UM samples, and $TP53^{dis}$ CLL included 6 IGHV M and 6 IGHV UM samples. A representative blot is shown, together with UPN and cumulative band intensity data obtained from the analysis of the four subsets. Box plots represent median value and 25%-75% percentiles, whiskers represent minimum and maximum values of band intensity for each group. Vertical lines have been inserted to indicate repositioned gel lanes. **** p<0.0001, ** p<0.01.

Supplemental Figure 3

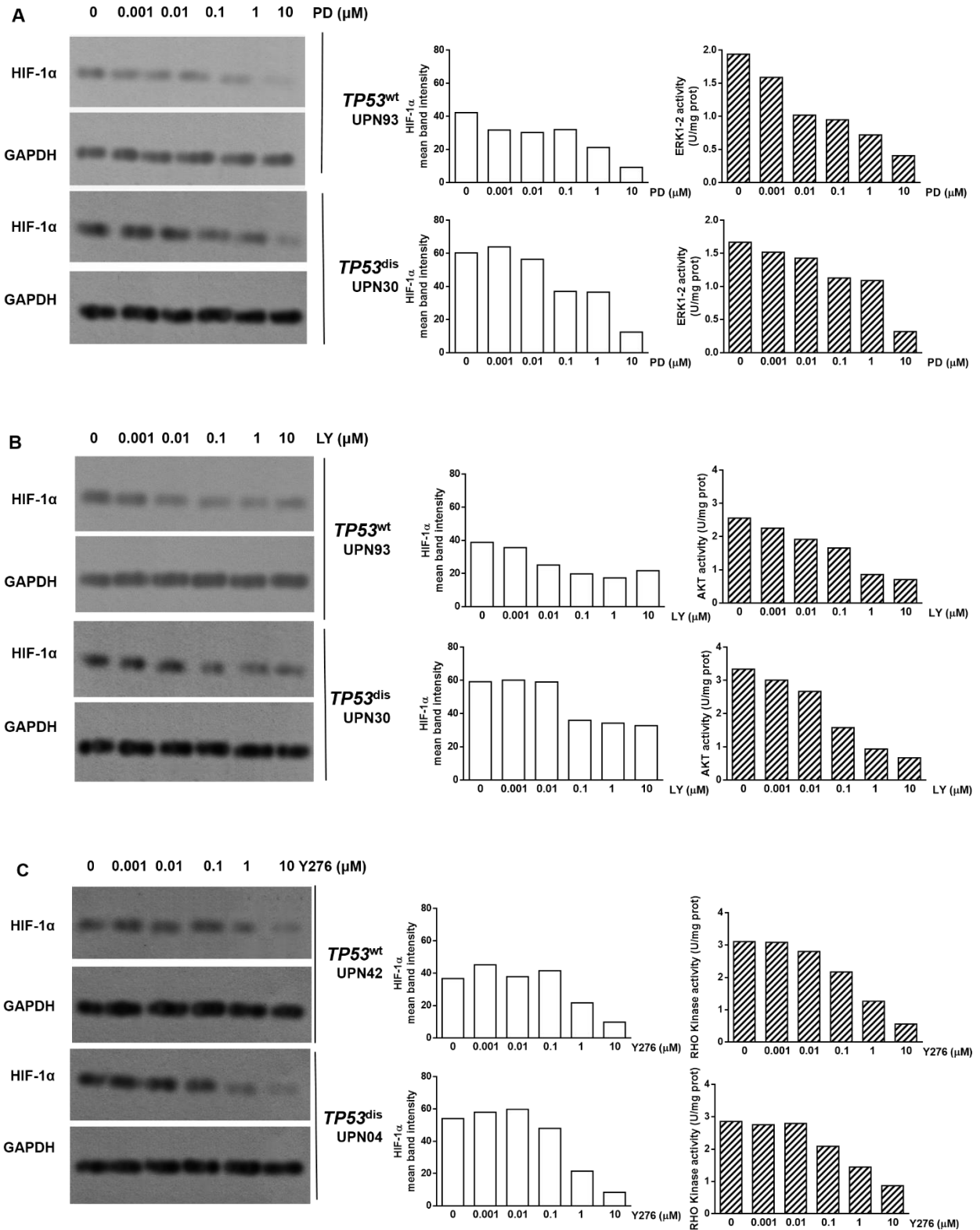


Figure S3. Increasing concentrations of ERK1-2, PI3K or RHOA kinase inhibitors determine a progressive reduction of HIF-1 α levels. Primary CLL cells were cultured for 48 hours in the presence of increasing concentration of PD98059 (PD, 0.01 μ M, 0.1 μ M, 1 μ M or 10 μ M) **(A)**, LY294002 (LY, 0.01 μ M, 0.1 μ M, 1 μ M or 10 μ M) **(B)** or Y27632 (Y276 0.01 μ M, 0.1 μ M, 1 μ M or 10 μ M) **(C)**. WB analyses of HIF-1 α protein expression for 1 *TP53*^{wt} and 1 *TP53*^{dis} representative CLL patient, together with UPN and the corresponding cumulative band intensity data, are shown. ERK1-2, AKT and RHOA kinase activities were evaluated by an immunomediated assay and are shown by bar graphs on the right.

Supplemental Figure 4

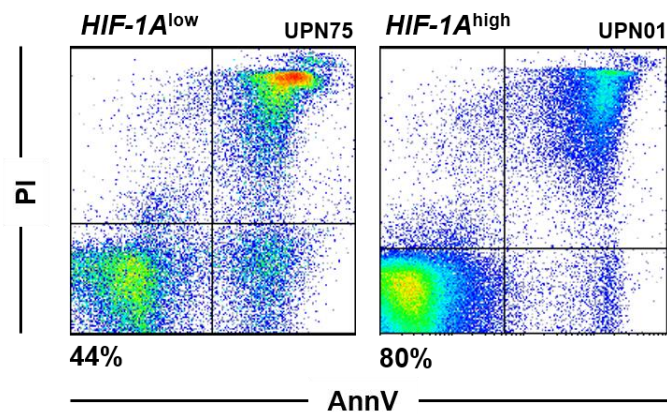


Figure S4. Viability of *HIF-1A*^{high} and *HIF-1A*^{low} CLL cells. Representative flow cytometry analysis (relative UPN indicated) of AnnV/PI expression on *HIF-1A*^{high} and *HIF-1A*^{low} CLL cells after 48-hour culture in medium. CLL cells isolated from *HIF-1A*^{high} samples had a significantly higher viability than CLL cells isolated *HIF-1A*^{low} samples.

Supplemental Figure 5

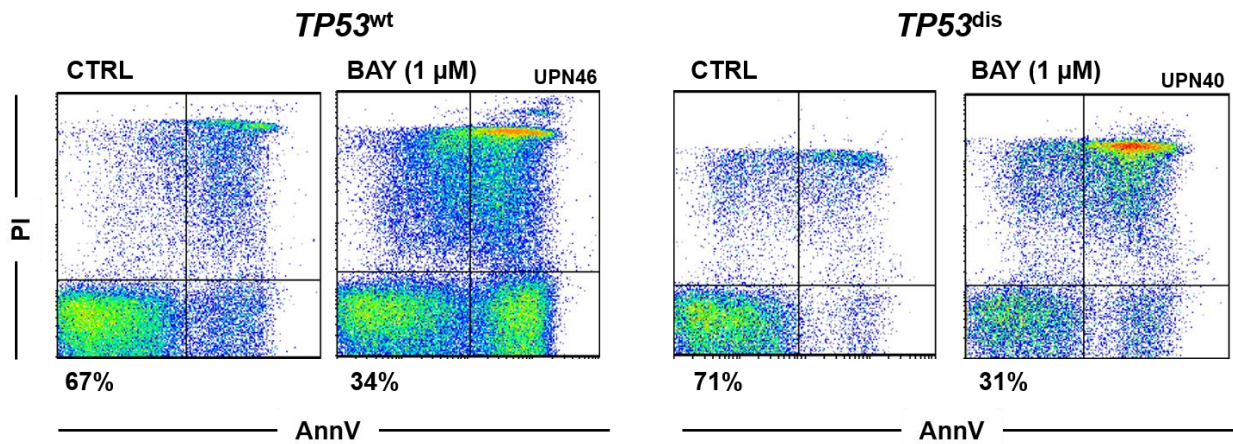


Figure S5. Viability of $TP53^{wt}$ and $TP53^{dis}$ CLL cells exposed to BAY87-2243. Representative flow cytometry analysis (relative UPN indicated) of AnnV/PI expression on $TP53^{wt}$ and $TP53^{dis}$ CLL cells exposed to 1 μ M BAY87-2243 (BAY) or left untreated for 48 hours. BAY87-2243 determined a direct cytotoxic effect toward leukemic cells isolated from both patient subsets.

Supplemental Figure 6

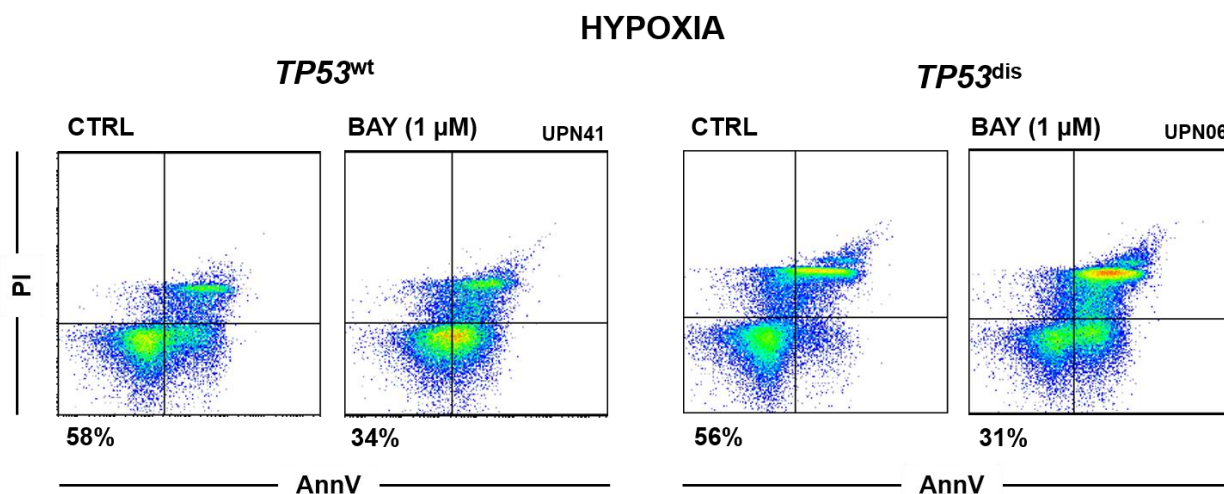


Figure S6. Viability of $TP53^{wt}$ and $TP53^{dis}$ CLL cells exposed to BAY87-2243 under hypoxia. Representative flow cytometry analysis (relative UPN indicated) of AnnV/PI expression on $TP53^{wt}$ and $TP53^{dis}$ CLL cells exposed to 1 μ M BAY87-2243 (BAY) or left untreated for 48 hours, under hypoxic conditions. BAY87-2243 exerted a cytotoxic effect also when $TP53^{dis}$ and $TP53^{wt}$ CLL cells were cultured in conditions of hypoxia.

Supplemental Figure 7

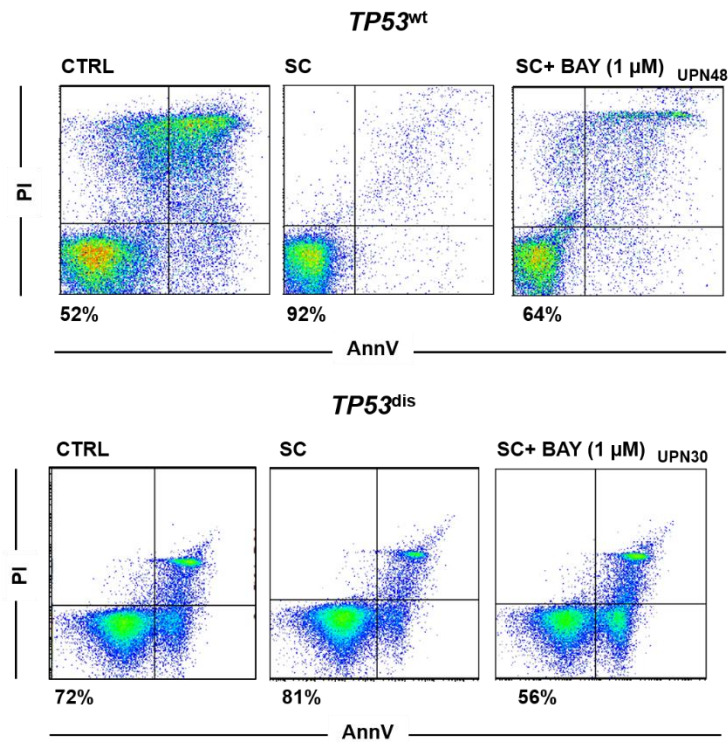


Figure S7. Viability of $TP53^{wt}$ and $TP53^{dis}$ CLL cells exposed to BAY87-2243 in presence of SC. Representative flow cytometry analysis (relative UPN indicated) of AnnV/PI expression on $TP53^{wt}$ and $TP53^{dis}$ CLL cells exposed to 1 μ M BAY87-2243 (BAY) or left untreated for 48 hours, in the presence or in the absence of the murine SC line M2-10B4. BAY87-2243 exerted a cytotoxic effect also when $TP53^{dis}$ and $TP53^{wt}$ CLL cells were co-cultured with SC.

Supplemental Figure 8

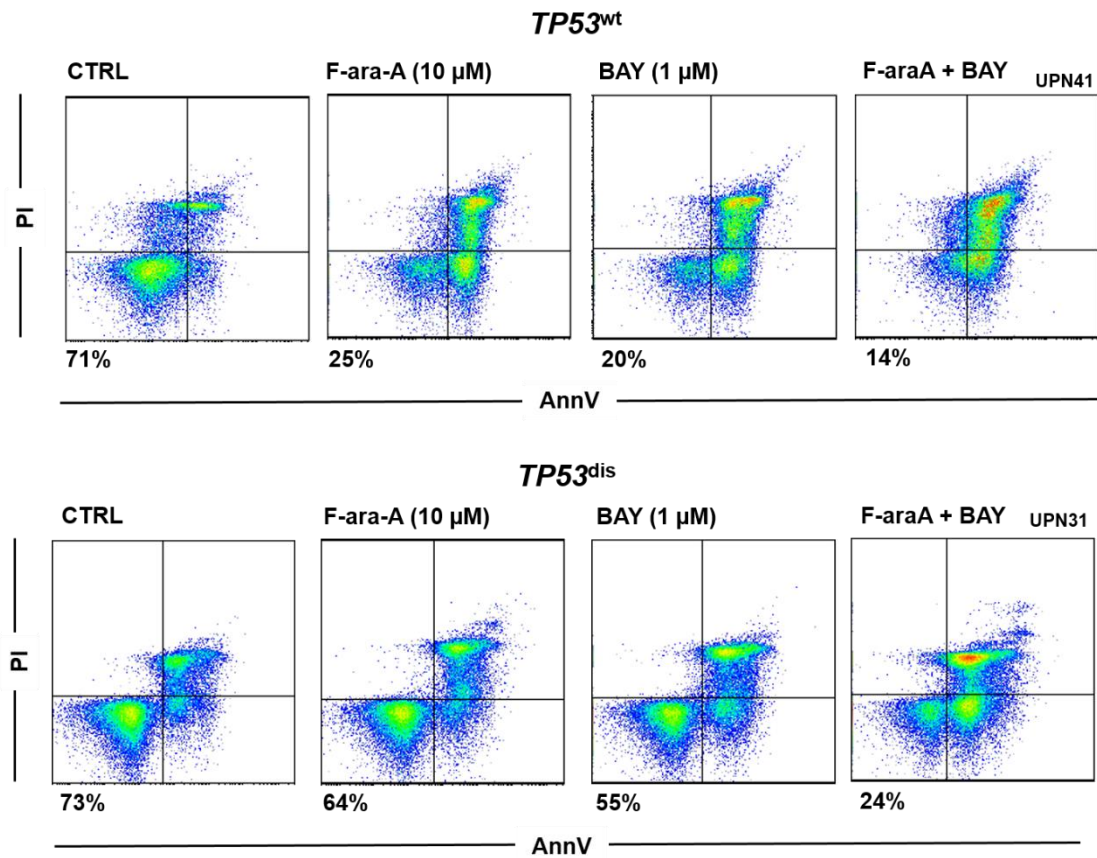


Figure S8. Viability of TP53^{wt} and TP53^{dis} CLL cells exposed to BAY87-2243 + fludarabine. Representative flow cytometry analysis (relative UPN indicated) of AnnV/PI expression on TP53^{dis} and TP53^{wt} CLL cells exposed for 48 hours to 1 μ M BAY87-2243 (BAY) and/or 10 μ M F-ara-A. The combination BAY87-2243 + F-ara-A determined a significant decrease in the viability of TP53^{wt} and TP53^{dis} CLL cells, compared to each compound used as single agent and to untreated controls.

Supplemental Figure 9

F-ara-A (μ M)		<i>TP53</i> ^{wt}				<i>TP53</i> ^{dis}			
BAY (μ M)		0.01	0.1	1	10	0.01	0.1	1	10
0.01		1.58	6.9	0.28	1.1	57.5	1.44	0.36	0.56
0.1		0.44	0.58	0.29	1.21	0.67	0.08	0.1	0.24
0.5		0.67	1.74	0.24	0.92	0.76	2.8	0.48	0.35
1		1.53	0.73	0.38	0.62	6.66	0.65	0.18	0.17

Combination Index

Figure S9. CI of BAY87-2243 + fludarabine combinations. Figure showing combination indexes (CI) relative to 48-hour treatment with BAY87-2243 (BAY) and F-ara-A, used at different concentrations in *TP53*^{wt} and *TP53*^{dis} CLL cells. CI<1, highlighted in bold, indicate synergistic combinations.

Supplemental Figure 10

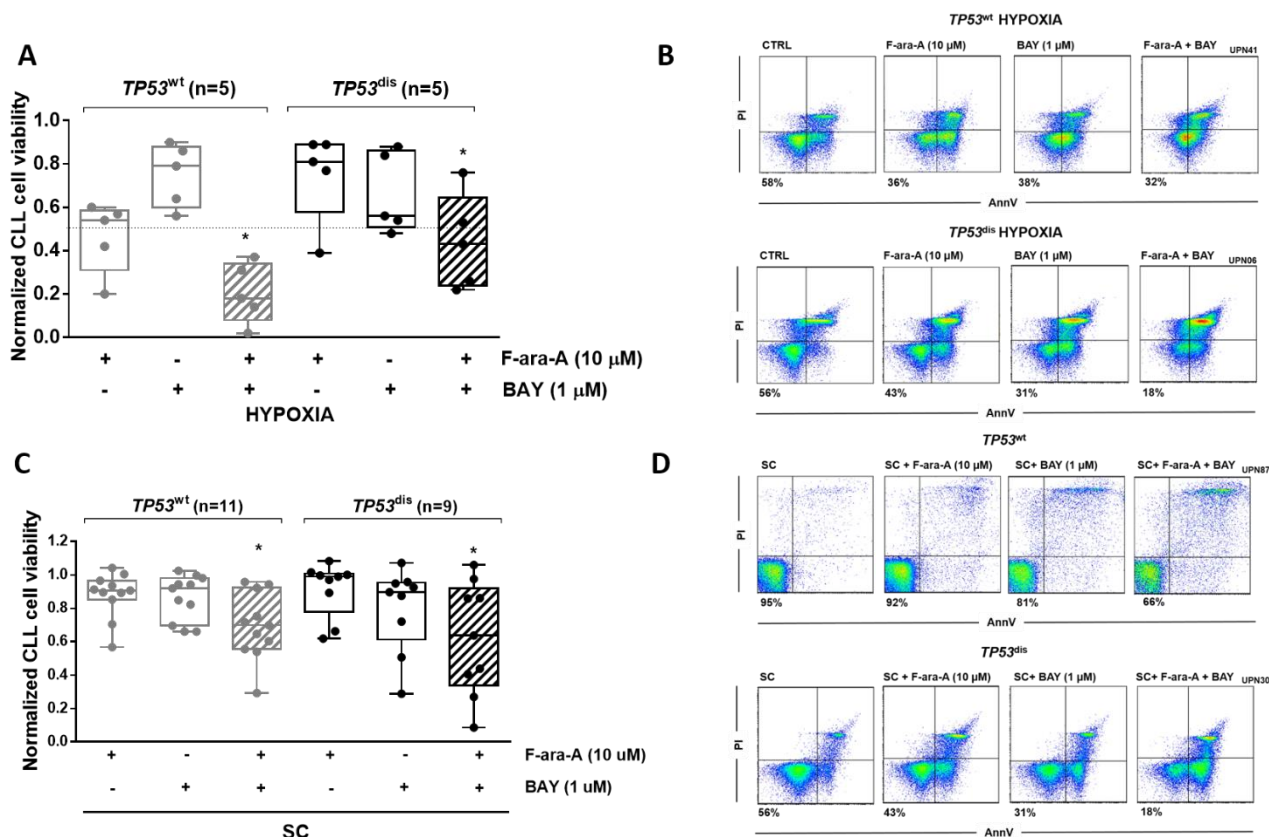


Figure S10. BAY87-2243 + fludarabine combination exerts a significant cytotoxic effect on $TP53^{dis}$ and $TP53^{wt}$ CLL cultured under hypoxia or in the presence of SC. Normalized cell viability of $TP53^{dis}$ and $TP53^{wt}$ CLL cells exposed for 48 hours to 1 μ M BAY87-2243 (BAY) and/or 10 μ M F-ara-A, under normoxia and hypoxia, or in co-culture with SC. The combination BAY87-2243 + F-ara-A (striped pattern) determined a significant decrease in the viability of $TP53^{wt}$ and $TP53^{dis}$ CLL cells, compared to each compound used as single agent, in condition of hypoxia (**A**, **B**) or in the presence of SC (**C**, **D**). In panels A and C, box plots represent median values and 25%-75% percentiles, whiskers represent minimum and maximum values for each group, together with all the points. In panels B and D, representative flow cytometry analysis (relative UPN indicated) of

AnnV/PI expression on TP53^{dis} and TP53^{wt} CLL cells exposed for 48 hours to 1 μ M BAY87-2243 and/or 10 μ M F-ara-A in the presence of SC.

Supplemental Figure 11

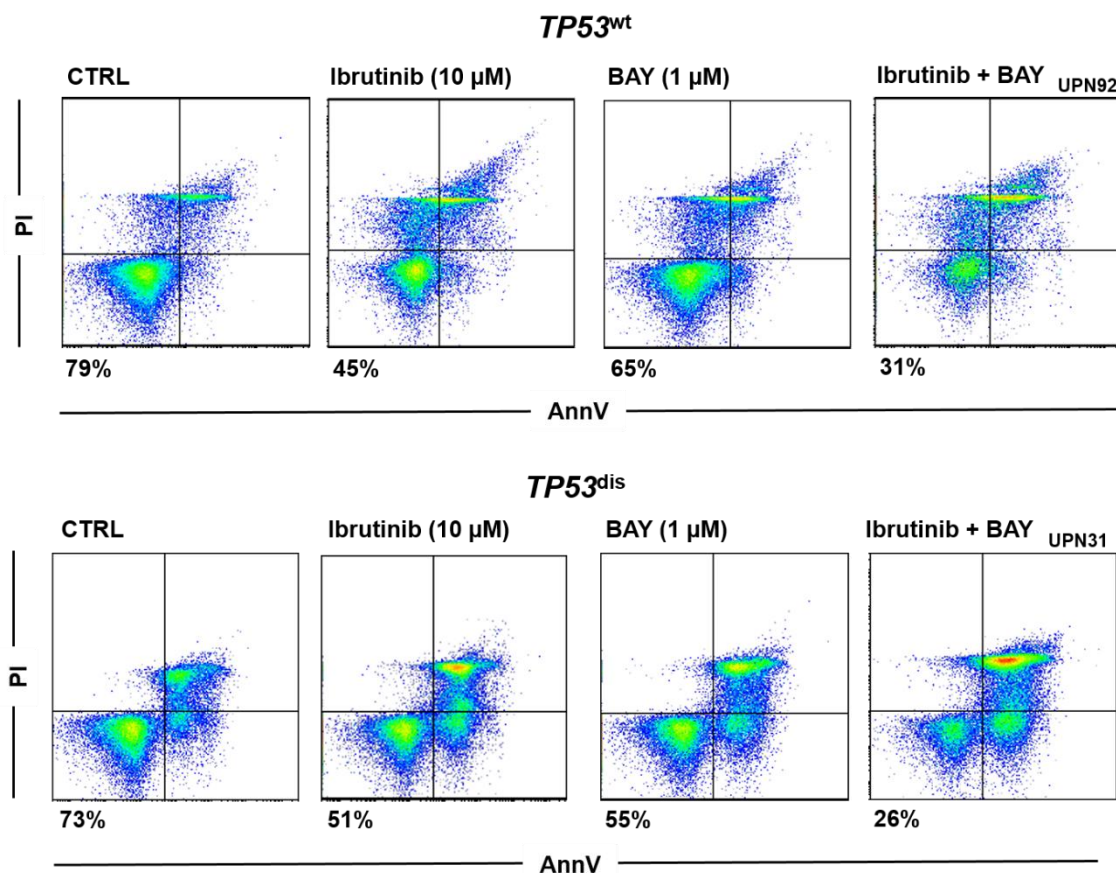


Figure S11. Viability of *TP53*^{wt} and *TP53*^{dis} CLL cells exposed to BAY87-2243 + ibrutinib. Representative flow cytometry analysis (relative UPN indicated) of AnnV/PI expression on *TP53*^{dis} and *TP53*^{wt} CLL cells exposed for 48 hours to 1 μ M BAY87-2243 (BAY) and/or 10 μ M ibrutinib. The combination BAY87-3342 + ibrutinib determined a significant decrease in the viability of *TP53*^{wt} and *TP53*^{dis} CLL cells, compared to each compound used as single agent and to untreated controls.

Supplemental Figure 12

Ibrutinib (μ M)	<i>TP53</i> ^{wt}				<i>TP53</i> ^{dis}			
	0.01	0.1	1	10	0.01	0.1	1	10
0.01	0.03	0.07	0.18	0.08	0.07	0.08	0.34	0.55
0.1	0.04	0.07	0.03	0.01	0.16	0.04	0.22	0.28
0.5	0.27	0.1	0.06	0.03	0.21	0.27	1.17	0.48
1	0.3	0.2	0.33	0.02	0.33	0.1	0.21	0.25

Combination Index

Figure S12. CI of BAY87-2243 + ibrutinib combinations. Figure showing combination indexes (CI) relative to the 48-hour treatment with BAY87-2243 (BAY) and ibrutinib, used at different concentrations in *TP53*^{wt} and *TP53*^{dis} CLL cells. CI<1, highlighted in bold, indicate synergistic combinations.

Supplemental references

1. Ricca I, Rocci A, Drandi D, et al. Telomere length identifies two different prognostic subgroups among VH-unmutated B-cell chronic lymphocytic leukemia patients. *Leukemia* 2007;21(4):697–705.
2. Rigoni M, Riganti C, Vitale C, et al. Simvastatin and downstream inhibitors circumvent constitutive and stromal cell-induced resistance to doxorubicin in IGHV unmutated CLL cells. *Oncotarget* 2015;6(30):29833–29846.